Esomeprazole affects the proliferation, metastasis, apoptosis and chemosensitivity of gastric cancer cells by regulating lncRNA/circRNA-miRNA-mRNA ceRNA networks

QIAN XU[1], XIYUN JIA[1], QIAN WU[2], LEI SHI[3], ZIHAN MA[1],
NAN BA[1], HAN ZHAO[1], XINGZHOU XIA[4] and ZISEN ZHANG[1]

[1]Department of Oncology, The Fifth Affiliated Hospital of Zhengzhou University, Zhengzhou,
Henan 450052; [2]Department of Gastroenterology, Huanghe Central Hospital, Zhengzhou,
Henan 450003; Departments of [3]Clinical Pharmacy and [4]Gastroenterology,
The Fifth Affiliated Hospital of Zhengzhou University, Zhengzhou, Henan 450052, P.R. China

Abstract. Recently, proton pump inhibitors have become a hot research topic in the field of cancer drug research. However, the specific anti-tumor effect and underlying mechanisms of esomeprazole (ESO) in gastric cancer (GC) have remained elusive. In the present study, the toxic effects of ESO on the GC cell line AGS were investigated. MTT assays confirmed that ESO inhibited the proliferation of AGS cells and significantly enhanced their chemosensitivity. Transwell assays were performed to determine the anti-metastatic effects of ESO in AGS cells. Flow cytometry demonstrated that ESO induced cell apoptosis and caused cell cycle arrest in the S and G2/M phases. Furthermore, the differential expression of 948 long non-coding RNAs (lncRNAs), 114 circular RNAs (circRNAs), 1,197 mRNAs and 199 microRNAs (miRNAs) was detected in AGS cells via microarray analysis and RNA-sequencing. The top 10 differently expressed genes were mostly located on chromosomes 10 and 19. In addition, Gene Ontology analysis indicated that the genes were accumulated in functional terms associated with DNA replication, the cell cycle and the apoptotic signaling pathway. Kyoto Encyclopedia of Genes and Genomes pathway analysis revealed a variety of significantly dysregulated signaling pathways and targets, including the EGFR tyrosine kinase inhibitor resistance pathway, forkhead box O signaling pathway, p53 signaling pathway and platinum drug resistance pathway. Subsequently, the interactions of microtubule-associated protein 2 (MAP2), homeodomain-interacting protein kinase 2 (HIPK2) and ankyrin 2 (ANK2) were noted in a competing endogenous RNA (ceRNA) network, which may be important targets of ESO, exerting an anti-tumor effect in AGS cells. Collectively, ESO affects the proliferation, metastasis, apoptosis and chemosensitivity of gastric cancer cells by regulating long non-coding RNA/circRNA-miRNA-mRNA ceRNA networks.

Introduction

Gastric cancer (GC) is the fifth most common cancer type and ranks as the second leading cause of cancer-associated death worldwide (1). Due to the lack of distinct symptoms at the early stage, the majority of patients are diagnosed in advanced stages and lose the opportunity of radical surgery, and chemotherapy-based treatment remains the main strategy. However, no remarkable advances were achieved in the past decades (2). With the developments in molecular biology, certain molecular targets were discovered, which have been successfully used in the treatment of tumors (3,4). However, the prospect of targeted therapy for GC remains uncertain and the underlying obstacle may be the lack of effective molecular targets. Therefore, it is urgent to explore novel mechanisms of anti-GC drugs and provide new targets in order to improve the prognosis of GC.

Proton pump inhibitors (PPIs) such as benzimidazole derivatives, are safely used to treat a wide range of gastrointestinal disorders such as peptic ulcer, gastritis and reflux esophagitis (5). Depending on their structure and chemical properties, PPIs may have different mechanisms of action. Recently, PPIs have been repurposed, including their application to decrease cisplatin-induced nephrotoxicity, target viral replication and inhibit the thioesterase activity of human fatty acid synthase (6-8). In addition, PPIs have demonstrated anti-tumor activity in a variety of tumor types and the antitumor mechanism may be associated with apoptosis, autophagy and the acidic microenvironment (9). Esomeprazole (ESO), which is well known as a powerful stomach acid inhibitor, has been recently investigated regarding its growth inhibition,

Correspondence to: Dr Zisen Zhang or Dr Nan Ba, Department of Oncology, The Fifth Affiliated Hospital of Zhengzhou University, 3 Kangfu Front Street, Jingguang Road, Zhengzhou, Henan 450052, P.R. China
E-mail: zszhang@zzu.edu.cn
E-mail: bananbanana@163.com

drug synergy and drug resistance reversal functions in cancer cells (10,11). Due to limited research, the anti-tumor effect and mechanisms of action of ESO in GC cells have remained elusive.

Long non-coding RNAs (lncRNAs) are defined as autonomously transcribed non-coding RNAs longer than 200 nucleotides with no coding function. lncRNAs have various roles, such as remodeling of chromatin and genome architecture, RNA stabilization and transcriptional regulation (12). Circular RNAs (circRNAs) are a new type of endogenous noncoding RNA with a closed circular structure, which regulate linear RNA transcription, downstream gene expression and protein production (13). MicroRNAs (miRNAs or miRs) either inhibit mRNA translation or trigger mRNA degradation by binding to complementary sequences in the 3'-untranslated regions of their target mRNAs (14). lncRNAs and circRNAs may act as competing endogenous RNAs (ceRNAs) to control miRNA translation (15-17). lncRNAs, together with circRNAs, miRNAs, mRNAs and their interactions, provide insight into the molecular pathogenesis of GC and a novel direction for therapeutic approaches for this disease (17). Therefore, it is worthwhile to explore the underlying molecular mechanisms and targets (among lncRNAs, circRNAs, miRNAs and mRNAs) of ESO as a promising antitumor agent in GC cells.

The present study investigated the effects of ESO on the proliferation, metastasis, apoptosis and chemosensitivity in AGS cells. The differential expression profiles were determined using chip analysis and RNA-sequencing. Furthermore, an integrative network analysis among lncRNAs, circRNAs, miRNAs and mRNAs, was performed using bioinformatics methods.

Materials and methods

Cell line and cell culture. The human gastric cancer cell line AGS was provided by the Shanghai Cell Bank of the Chinese Academy of Sciences. Cells were cultured in F-12K medium (Hyclone; Cytiva) supplemented with 10% FBS (Hangzhou Sijiqing Biological Engineering Materials, Co., Ltd.) and antibiotics (100 U/ml penicillin and 100 μg/ml streptomycin) in humidified air with 5% CO_2 at 37˚C.

Proliferation assays. Cell proliferation assays were performed with MTT (Sigma-Aldrich; Merck KGaA). AGS cells were seeded into 96-well plates in 100 μl F-12K medium containing 10% FBS at a density of 1×10^4 cells per well and incubated overnight for cell attachment. Next, the cells were treated with ESO (AstraZeneca), adriamycin (ADM; Pfizer, Inc.) and cisplatin (DDP; Qilu Pharmaceutical Co., Ltd.), for 24 or 48 h. MTT solution (20 μl per well) was then added and the plate was incubated at 37˚C for an additional 4 h. Next, the medium was discarded and 150 μl DMSO was added to each well, followed by incubation for 10 min until the formazan crystals that had formed were completely dissolved. The absorbance was measured at 490 nm using a microplate reader (BioTek Instruments, Inc.).

Transwell assays. The assays were performed in Transwell insert chambers (pore size, 8 μm; Corning, Inc.). Approximately 1×10^5 cells treated with ESO (0, 10, 20 and 40 μg/ml) alone, or combined with ADM (0.2 μg/ml) or DDP (20 μg/ml), were seeded into the upper chamber in serum-free medium in triplicate with or without Matrigel (BD Biosciences) for the invasion and migration assay, respectively. A total of 600 μl F-12K medium with 10% FBS was added to the lower chamber. After incubation with the above drugs for 12 h, the upper chambers were fixed with 4% paraformaldehyde for 30 min at 37˚C, and then stained with 0.1% crystal violet for 30 min at 37˚C. The migrating and invading cells were counted in at least 6 visual fields per membrane under a light microscope (Olympus Corp.).

Flow cytometric analysis. In brief, 2×10^5 cells in 500 μl serum-free medium were seeded into 24-well plates and treated with ESO (10 μg/ml) alone or in the presence of ADM (0.05 μg/ml) or DDP (2.5 μg/ml), for apoptosis analysis, while cells were treated with ESO (40 μg/ml) alone or in the presence of ADM (0.2 μg/ml) or DDP (20 μg/ml), for cell cycle analysis. After incubation at 37˚C for 12-48 h, the cells were collected for apoptosis and cell cycle analyses using an Annexin V-FITC/PI apoptosis assay kit (BD Biosciences). The cells were stained with 400 μl 1X binding buffer and 5 μl Annexin V-FITC for 15 min, followed by incubation with 5 μl PI for 5 min at room temperature in the dark for the apoptosis assay. For cell cycle analysis, cells were fixed with ice-cold ethanol at 4˚C overnight and suspended in ice-cold PBS containing 50 μg/ml PI at room temperature for 30 min. The cells were immediately analyzed on an Accuri C6 flow cytometer (BD Biosciences).

Microarray assay. The microarray Agilent Human lncRNA V6 (Agilent Technologies, Inc.) was used. Total RNA extracted from the control and experimental group (0 and 40 μg/ml ESO treatment, respectively) was quantified with the NanoDrop ND-2000 (Thermo Fisher Scientific, Inc.) and the RNA integrity was assessed using an Agilent Bioanalyzer 2100 (Agilent Technologies, Inc.). Sample labeling, microarray hybridization and washing were performed based on the manufacturer's standard protocols. In brief, total RNA was transcribed into double-strand complementary (c)DNA, then reverse-transcribed into cRNA and labeled with cyanine-3-cytidine triphosphate. The labeled cRNAs were hybridized onto the microarray. After washing, the arrays were scanned with an Agilent Scanner G2505C (Agilent Technologies, Inc.).

Feature Extraction software (version 10.7.1.1; Agilent Technologies, Inc.) was used to analyze array images to obtain raw data. GeneSpring (version 13.1; Agilent Technologies, Inc.) was employed to normalize the raw data with the quantile algorithm. Differentially expressed genes (DEGs) or transcripts were identified through fold-change and P-value as calculated with Student's t-test. The threshold set for up- and downregulated genes or transcripts was fold change >2.0 and P<0.05.

RNA-sequencing. The preparation of whole-transcriptome libraries and deep sequencing were performed by Illumina analysis (Shanghai OE Biotech Co., Ltd.). For primary analysis, the length distribution of the RNA sequences in the reference genome (ftp://ftp.ncbi.nlm.nih.gov/genomes) was determined. The known miRNAs were identified by alignment against the miRBase v.21 database (http://www.mirbase.org/) and patterns

in different samples were analyzed. Unannotated small RNAs were analyzed by the software miRDeep2 (version 0.0.8; GitHub, Inc.) to predict novel miRNAs.

Functional enrichment analysis. Functional enrichment analysis was performed with the Database for Annotation, Visualization and Integrated Discovery (DAVID; https://david.ncifcrf.gov/) to determine the roles of differentially expressed RNAs. Gene Ontology (GO) analysis was performed to obtain significantly enriched terms in order to deduce important biological functions involving multiple RNAs. Furthermore, Kyoto Encyclopedia of Genes and Genomes (KEGG) pathway analysis was used to identify the likely functions and pathways associated with DEGs.

Construction of a ceRNA regulatory network. The overlapped regions of the miRNA sequence binding sites both on lncRNAs/circRNAs and mRNAs were searched to predict lncRNA/circRNA-miRNA-mRNA interactions with the software miRanda v3.3a (http://www.microrna.org). The ceRNA networks were performed using Cytoscape (version 3.6.1; http://cytoscape.org/).

Statistical analysis. Values are expressed as the mean ± standard deviation from at least three independent determinations. One-way ANOVA followed by Bonferroni's post hoc test was used for multiple comparisons. Comparisons between two groups were performed with two-tailed Student's t-tests. All statistical analyses were performed using SPSS v21.0 (IBM Corp.). The plotting of all statistical graphs was performed with GraphPad Prism 8.0 (GraphPad Software, Inc.). $P<0.05$ was considered to indicate a statistically significant difference.

Results

ESO inhibits proliferation and metastasis, and increases chemosensitivity in AGS cells. MTT assays were performed to clarify whether ESO exerted cytotoxic effects on AGS cells. The results indicated that ADM, DDP and ESO significantly inhibited cell proliferation (Fig. 1A-D). Furthermore, ESO enhanced the susceptibility of AGS cells to the cytotoxic effects of ADM and DDP (Fig. 1E and F). The additional cytotoxic effect of ESO when combined with ADM and DDP was dose- and time-dependent. To further determine the effects of ESO, Transwell assays were performed (Fig. 1G and H). As expected, the migration and invasion abilities of AGS cells were markedly suppressed in a dose-dependent manner when the cells were treated with ESO, either alone or in combination with ADM or DDP. In addition, the combination of the above three drugs displayed a lower metastasis potential compared with that caused by the combination of two drugs. These results suggested that ESO suppressed proliferation and metastasis, and enhanced chemosensitivity of AGS cells.

ESO induces AGS cell apoptosis via causing cell cycle arrest at the S and G2/M phases. ESO induced AGS cell apoptosis, as demonstrated by flow cytometry (Fig. 2A). The apoptosis rates were significantly increased in AGS cells treated with ESO, ADM or DDP. Furthermore, when treating the cells with a combination of the above three drugs, the highest number of apoptotic cells was observed. Cell cycle analysis suggested that the proportion of cells in G0/G1 phase decreased significantly, while the proportion of cells in the S and G2/M phases increased after ESO treatment in a time-dependent manner (Fig. 2B). Different phenomena were observed when ADM and DDP were added to the cells, either alone or in combination with ESO. The numbers of cells arrested in S phase were markedly increased, while those in G0/G1 phase were significantly decreased (Fig. 2C-E). Taken together, the present results suggested that ESO induced AGS cell apoptosis, and caused cell cycle arrest in the S and G2/M phases in a time-dependent manner. In combination with ADM and DDP, ESO induced S-phase arrest in AGS cells.

Identification of differentially expressed lncRNAs, circRNAs, miRNAs and mRNAs. To further analyze DEGs involved in the regulatory effects of ESO on AGS cells, microarray analysis and RNA-sequencing were performed. A total of 948 lncRNAs (487 upregulated and 461 downregulated), 114 circRNAs (32 upregulated and 82 downregulated), 1,197 mRNAs (498 upregulated and 699 downregulated) and 199 miRNAs (71 upregulated and 128 downregulated) were identified to be differentially expressed with a fold change >2.0 and $P<0.05$ (Fig. 3A-F). The top 10 DEGs were distributed on multiple chromosomes (chrs), particularly chr10 and chr19. The top 10 upregulated and downregulated lncRNAs, circRNAs, miRNAs and mRNAs were identified from the microarrays (Tables SI-IV).

GO and KEGG pathway analyses. The results of the functional enrichment analysis suggested that upregulated lncRNAs were mainly involved in intrinsic apoptotic signaling pathway in response to endoplasmic reticulum stress (GO:0070059) in the category biological process (BP) (Fig. S1A). DNA replication, nucleosome and protein heterodimerization activity were the most meaningful downregulated terms in BP, cellular component (CC) and molecular function (MF), respectively (Fig. S1B). From the KEGG pathway analysis, EGFR tyrosine kinase inhibitor resistance [path: *Homo sapiens* (hsa)01521] and miRNAs in cancer were most significantly enriched by upregulated lncRNAs (Fig. S1C). However, cell cycle and DNA replication were the top pathways enriched by downregulated lncRNAs (Fig. S1D). As expected, regulation of transcription, DNA-templated and protein binding were the top terms associated with miRNAs in the categories BP and MF, respectively (Fig. 4). And hydrogen; potassium-exchanging ATPase complex (H^+, K^+-ATPase), positive regulation of sodium; potassium-exchanging ATPase (Na^+, K^+-ATPase) activity and regulation of ATPase activity were also noted from GO analysis (Table SV). Furthermore, KEGG analysis indicated that target genes of miRNAs were significantly enriched in the oxytocin signaling pathway and a larger number of target genes were associated with pathways in cancer (Fig. 5). Of note, the cell cycle and DNA replication were also highlighted in the lncRNA/circRNA-miRNA-mRNA ceRNA networks (Fig. 6). These results suggested that ESO exerted its anti-GC effect via those co-expression networks, impacting both lncRNAs and circRNAs associated with DNA replication and the cell cycle.
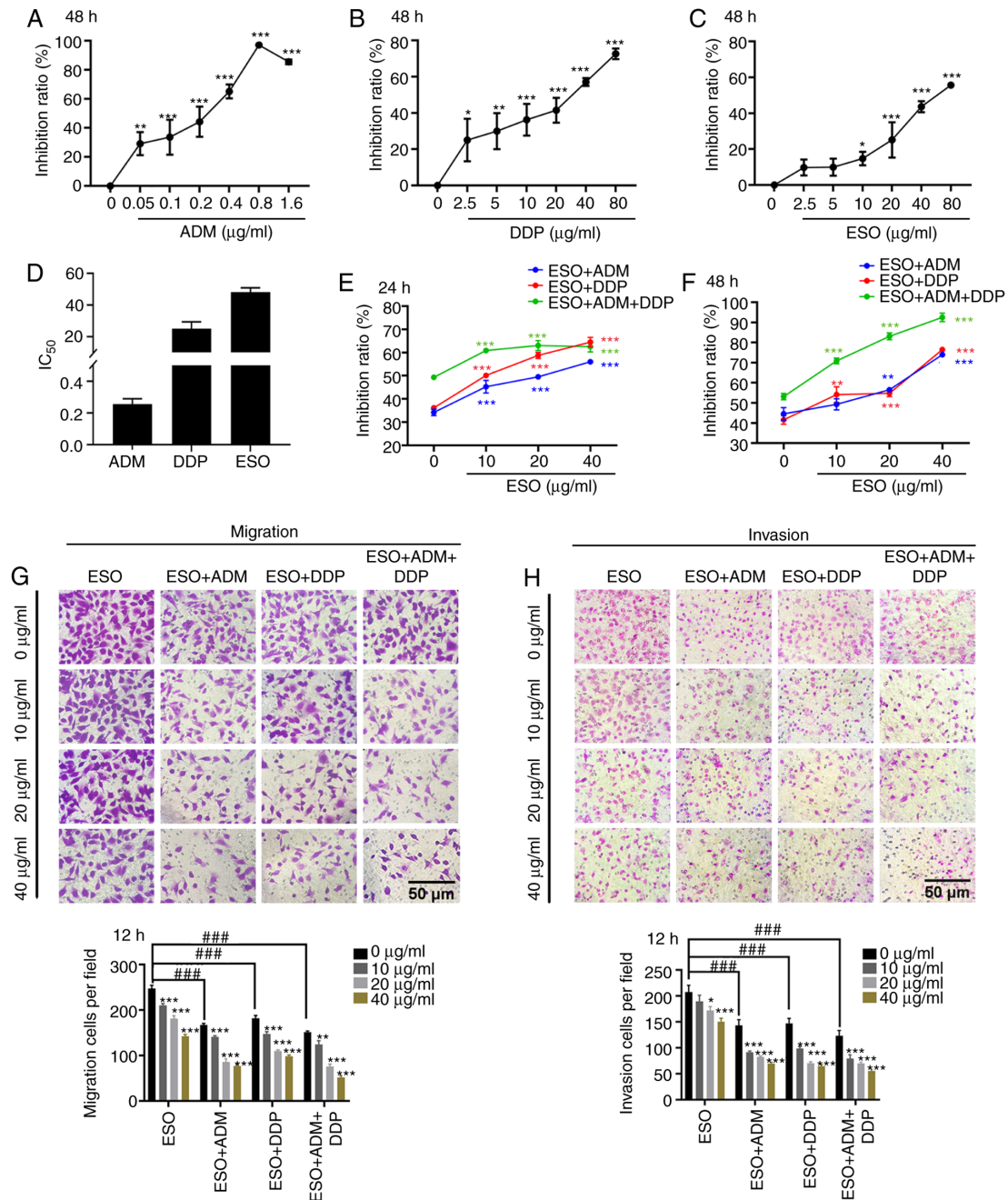
Figure 1. ESO inhibits proliferation and metastasis, and increases chemosensitivity in AGS cells. (A-C) MTT assays demonstrated that (A) ADM, (B) DDP and (C) ESO inhibited cell proliferation. (D) The IC_{50} of ADM, DDP and ESO in AGS cells. (E and F) ESO significantly increased chemosensitivity in AGS cells in a dose- and time-dependent manner (E) 24 h and (F) 48 h. (G and H) Transwell assays verified that ESO inhibited the (G) migration and (H) invasion of AGS cells, alone or in combination with 0.2 μg/ml ADM or 20 μg/ml DDP (scale bars, 50 μm). *P<0.05, **P<0.01 and ***P<0.001 vs. control; ###P<0.001 as indicated. ESO, esomeprazole; ADM, adriamycin; DDP, cisplatin; IC_{50}, half maximal inhibitory concentration.

Sub-pathway analysis in the lncRNA co-expression network. To investigate the antitumor mechanism of ESO in GC, four representative sub-pathways were selected through KEGG pathway analysis, including the EGFR tyrosine kinase inhibitor resistance pathway, FOXO signaling pathway, p53 signaling pathway and platinum drug resistance pathway. There were complex associations between mRNAs and multiple lncRNAs. The results indicated that upregulated vascular endothelial growth factor A (VEGFA), transforming growth factor α (TGFA), EGFR, FOXO3 and son of seven-less homolog (SOS)1, and downregulated fibroblast growth factor receptor 2 (FGFR2) and platelet-derived growth factor receptor α (PDGFRA), were associated with the EGFR tyrosine kinase inhibitors resistance signaling pathway (Fig. S2). Furthermore, certain genes, such as cyclin B1 (CCNB1), cyclin B2 (CCNB2) and S-phase kinase-associated protein 2 (SKP2) were downregulated, while other genes (FOXO3, EGFR, phosphatidylinositol 3-kinase, catalytic, 110-KD, α (PIK3CA) and SOS1) were upregulated in the FOXO signaling pathway (Fig. S3). Furthermore, the results demonstrated that lncRNAs regulated the development of GC after ESO treatment by targeting phorbol-12-myristate-13-acetate-induced
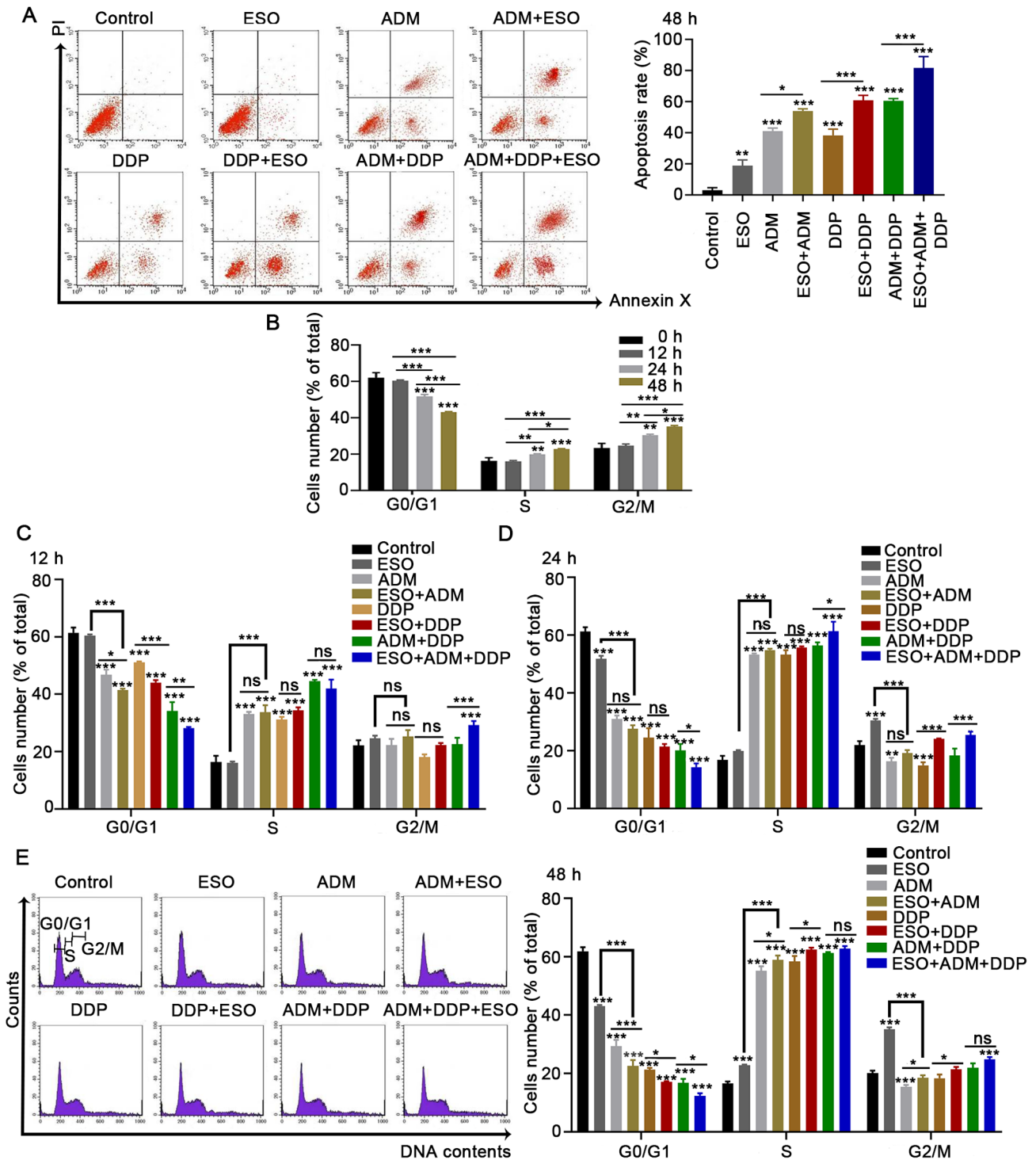
Figure 2. ESO induces AGS cell apoptosis by causing cell cycle arrest at the S and G2/M phases. (A) ESO induced AGS cell apoptosis, as analyzed by Annexin V-FITC/PI staining. (B) ESO caused cell cycle arrest at the S and G2/M phases in a time-dependent manner. (C-E) ESO combined with ADM and DDP induced S-phase arrest in AGS cells after incubation for (C) 12, (D) 24 and (E) 48 h. *P<0.05, **P<0.01 and ***P<0.001 vs. control. Ns, no significance; ESO, esomeprazole; ADM, adriamycin; DDP, cisplatin.

protein 1 (PMAIP1), cyclin-dependent kinase inhibitor 1A (CDKN1A), CCNB1 and CCNB2 in the p53 signaling pathway (Fig. S4). In addition, upregulation of CDKN1A, PMAIP1, mitogen-activated protein kinase kinase kinase-5 (MAP3K5), PIK3CA and downregulation of baculoviral inhibitor of apoptosis repeat containing 5 (BIRC5) were closely associated with the platinum drug resistance signaling pathway (Fig. S5).

Prediction of lncRNA/circRNA-miRNA-mRNA ceRNA network. In the present study, a total of 132,195 lncRNA-miRNA-mRNA ceRNA networks and 15,410 circRNA-miRNA-mRNA ceRNA networks were created using the differentially expressed lncRNAs (n=944), circRNAs (n=114), miRNAs (n=199) and mRNAs (n=939). The top lncRNAs and circRNAs regulating multiple miRNAs were highlighted, such as ENST00000261530, ENST00000281092 and
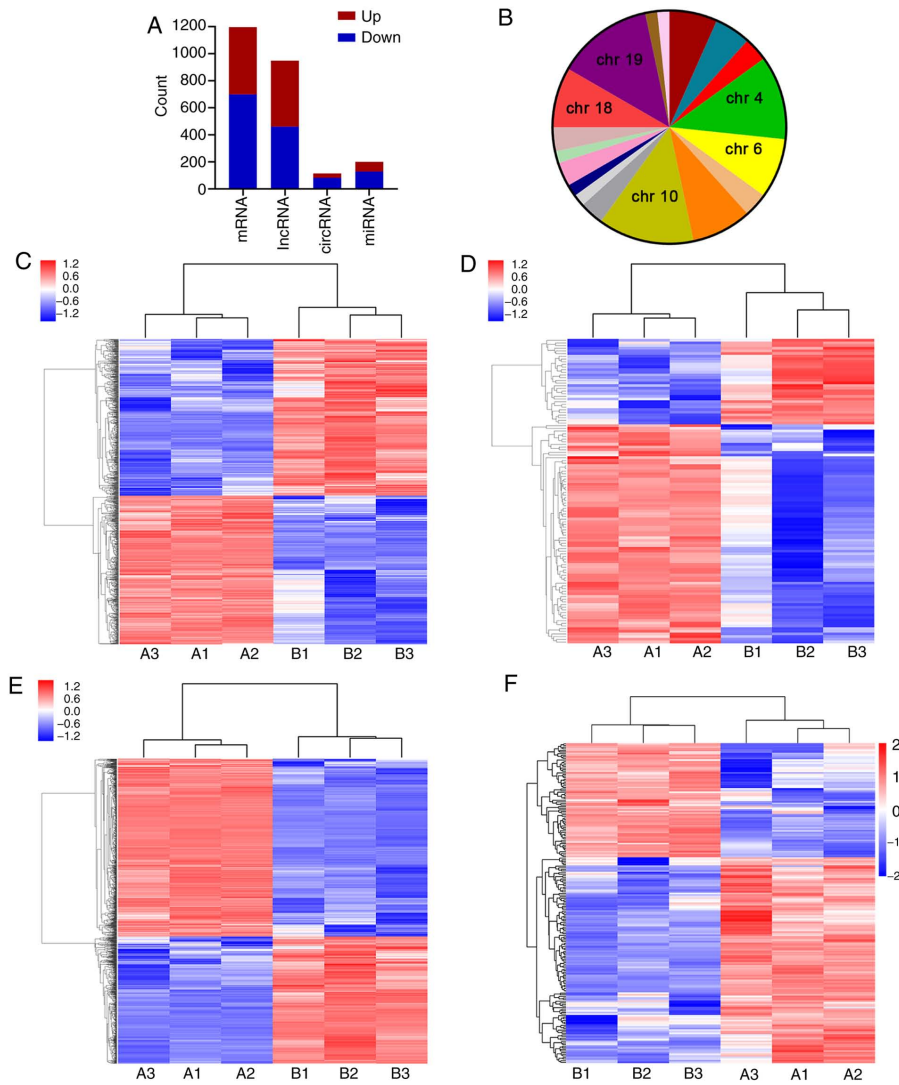
Figure 3. Differentially expressed genes and transcripts in AGS cells treated with ESO. (A) Statistical analysis of the results of differentially expressed genes and transcripts. (B) Chromosome distribution of the top 10 differentially expressed lncRNAs, circRNAs and mRNAs. Hierarchical clustering analysis of (C) lncRNAs, (D) circRNAs, (E) mRNAs and (F) miRNAs. Groups: A, control group; B, experimental group (40 µg/ml ESO). ESO, esomeprazole; chr, chromosome; lncRNA, long non-coding RNA; circRNA, circular RNA; miRNA, microRNA.
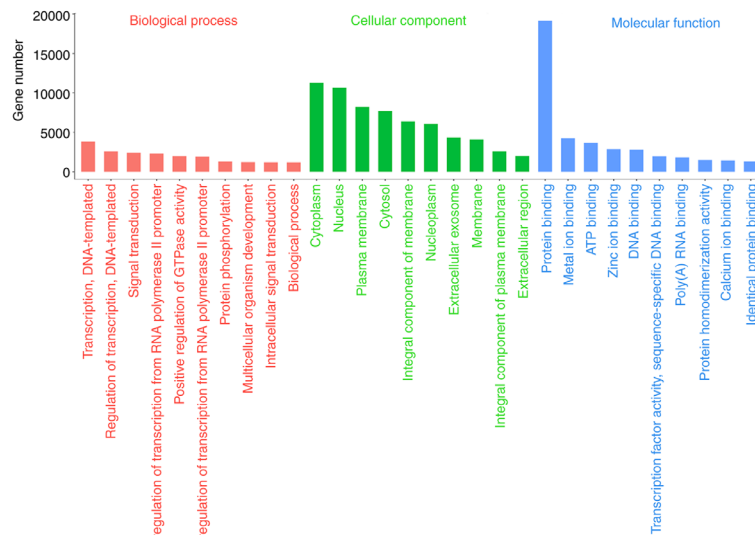

Figure 4. Enrichment analysis of differentially expressed microRNAs in the categories biological process, cellular component and molecular function.
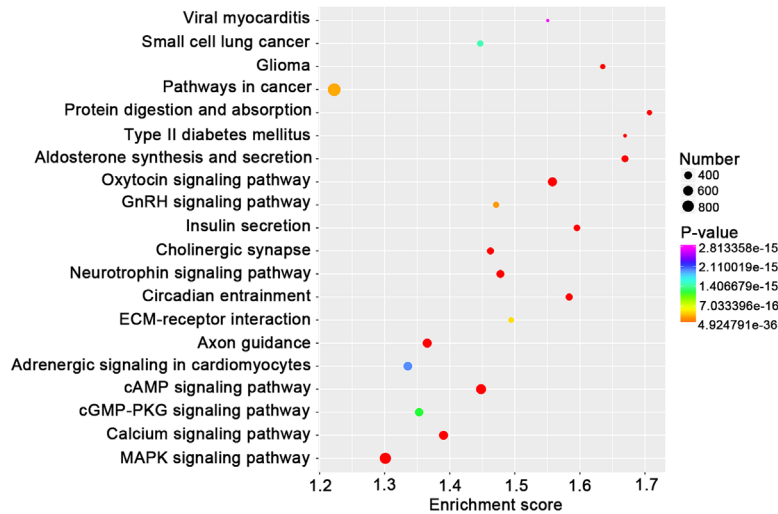
Figure 5. Top 20 most significantly enriched signaling pathways of differentially expressed microRNAs. Each bubble corresponds to a pathway. The bubble scale represents the number of differentially expressed genes. The color of the bubble represents the P-value. GnRH, gonadotropin-releasing hormone; ECM, extracellular matrix; cGMP, cyclic guanosine monophosphate; PKG, protein kinase G; MAPK, mitogen-activated protein kinases.
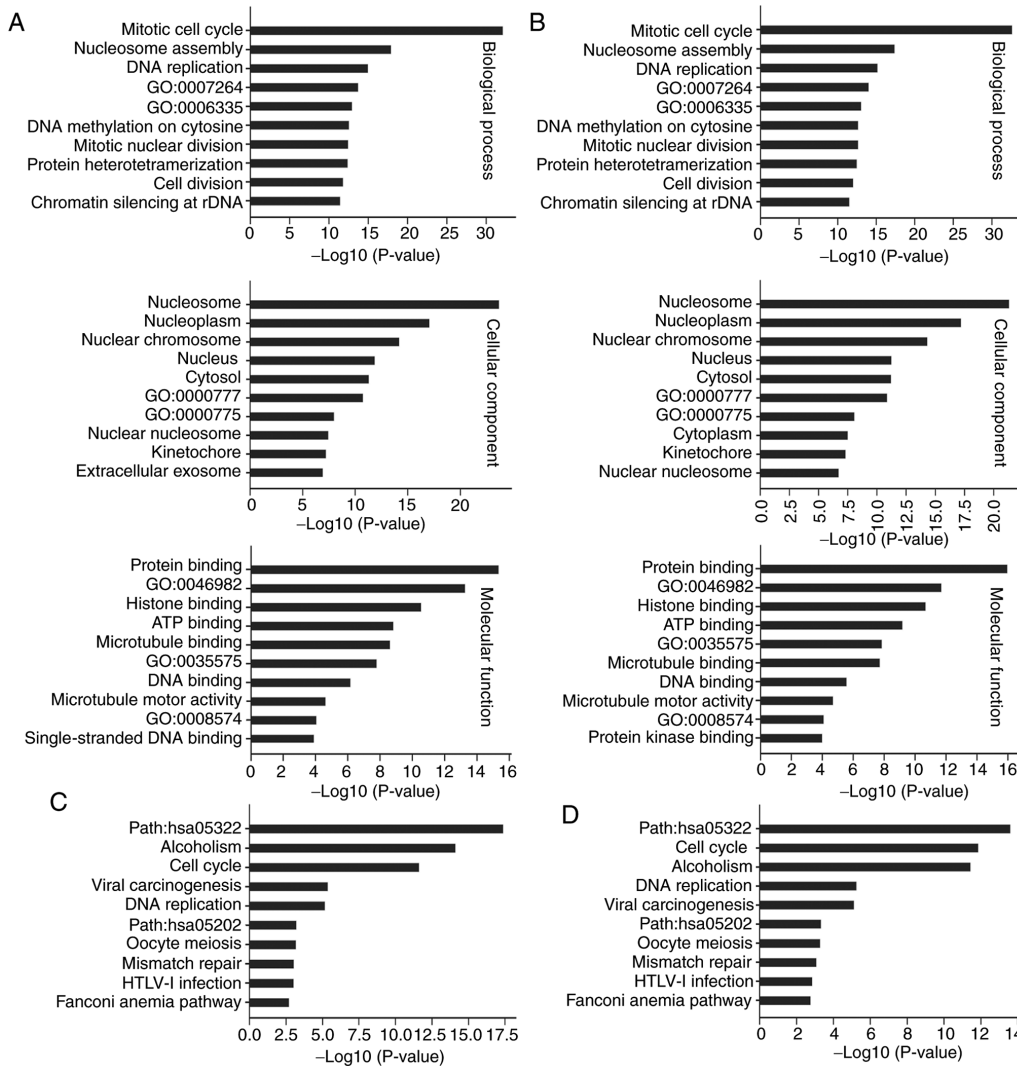

Figure 6. Functional enrichment analysis of components of the lncRNA/circRNA-miRNA-mRNA ceRNA network. (A and B) Enrichment analysis of the (A) lncRNA-miRNA-mRNA ceRNA network and the (B) circRNA-miRNA-mRNA ceRNA network in the GO terms biological process, cellular component and molecular function. (C and D) Top 10 most significantly enriched signaling pathways of the (C) lncRNA-miRNA-mRNA ceRNA and (D) circRNA-miRNA-mRNA ceRNA networks. lncRNA, long non-coding RNA; circRNA, circular RNA; miRNA, microRNA; ceRNA, competing endogenous RNA; GO, gene ontology; HTLV1, human T-cell leukemia virus type 1; rDNA, ribosomal DNA; hsa, Homo sapiens.
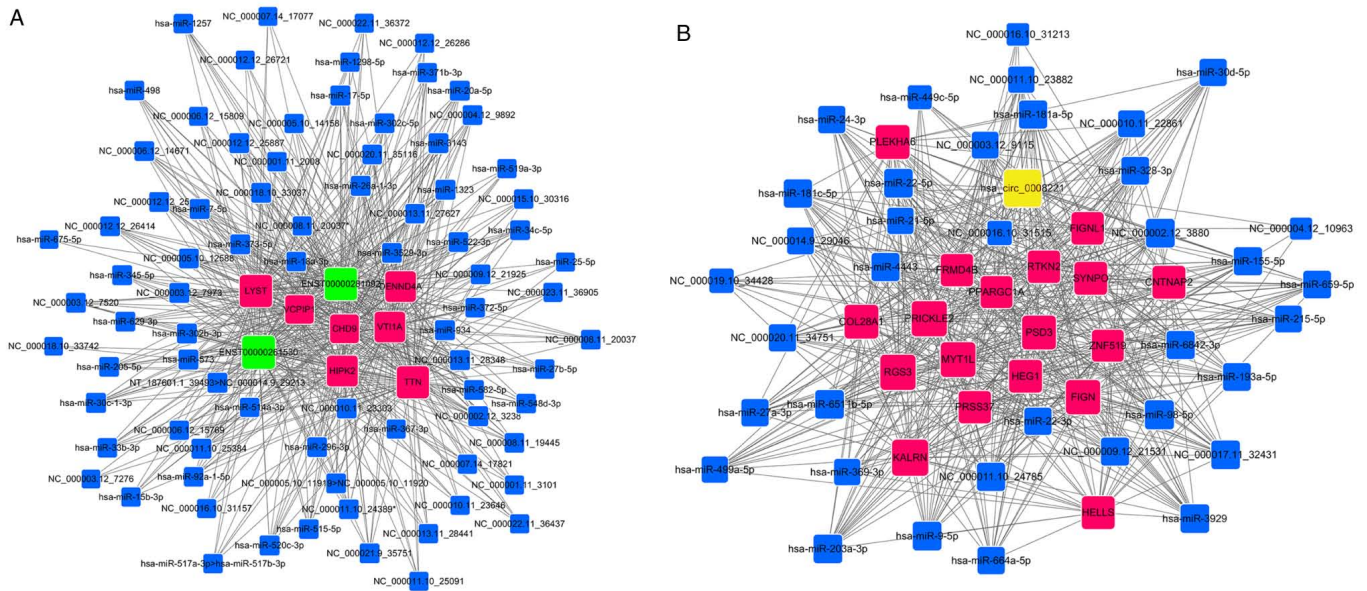
Figure 7. lncRNA/circRNA-miRNA-mRNA ceRNA network. (A) lncRNA-miRNA-mRNA ceRNA network. (B) circRNA-miRNA-mRNA ceRNA network. Green represents lncRNAs; yellow represents circRNAs; blue represents miRNAs; red represents mRNAs. ceRNA, competing endogenous RNA; lncRNA, long non-coding RNA; circRNA, circular RNA; miRNA, microRNA; hsa, *Homo sapiens*; ENST, the symbol of Ensembl ID.

hsa_circ_0008221, which may be defined as key nodes of the ceRNA network. There was a sub-network containing 2 lncRNAs, 81 miRNAs and 7 mRNAs (Fig. 7A). In addition, a ceRNA network consisted of 1 circRNA, 37 miRNAs and 18 mRNAs, as presented in Fig. 7B. Integrating of the lncRNA/circRNA-mRNA interactions indicated that microtubule-associated protein 2 (MAP2), homeodomain-interacting protein kinase 2 (HIPK2) and ankyrin 2 (ANK2) were targeted by both lncRNAs and circRNAs (Figs. S6 and S7). The list of data (Tables SVI and SVII) suggested that lncRNAs (NR_033268, ENST00000261530 and ENST00000281092) and circRNAs (hsa_circ_0076332 and hsa_circ_0059713) were the ceRNAs of hsa-miR-372-5p targeting MAP2, HIPK2 and ANK2. The above results revealed that the antitumor mechanism of ESO in GC may be mediated by lncRNA/circRNA-miRNA-mRNA ceRNA networks.

Discussion

It is well known that PPIs inhibit H^+ transport and disrupt the acidic microenvironment on tumors by inhibiting the activity of V-ATPase (a vacuolar proton pump), which is the pivotal basis for the anti-cancer mechanism of PPIs (9,11,18). In addition, growing evidence revealed that PPIs have numerous novel mechanisms responsible for their antitumor effects, including influencing intracellular signal transduction, chromatin remodeling, phosphorylation, autophagy and stress response (19-21). Subsequently, it was indicated that the mechanisms of PPIs to inhibit cell growth were closely associated with miRNAs. Omeprazole inhibited cell proliferation and induced cell cycle arrest through upregulating miR-203a-3p expression in Barrett's esophagus cells (22). Unexpectedly, ESO not only impacted the survival, metastatic potential and chemotherapy resistance of esophageal cancer cells, but also affected the expression of resistance-associated miRNAs (10). Furthermore, high doses of PPIs regulated the pathways associated with

tumor malignancy and the microenvironment via inhibiting the release of exosomes, which contain miRNAs (23). The present data suggested that ESO also affected the proliferation, metastasis, chemosensitivity and apoptosis of GC cells through regulating lncRNA/circRNA-miRNA-mRNA ceRNA networks.

In cytotoxicity assays, ESO inhibited cell proliferation and enhanced the susceptibility of the cells to ADM and DDP in a dose- and time-dependent manner. Furthermore, it significantly inhibited the migration and invasion of AGS cells in a dose-dependent manner. In addition, the inhibitory effect of ESO was more obvious when combined with ADM and DDP. The present results were consistent with those of previous studies (10,23). Thus, it was hypothesized that ESO suppressed the proliferation and metastatic potential, and increased the chemosensitivity of AGS cells in a dose-dependent manner.

Induction of apoptosis and cell cycle arrest are currently considered to be important mechanisms underlying the anticancer effects of potential drugs (22,24). The present results suggested that ESO significantly induced AGS cell apoptosis, which was enhanced after combination with ADM and DDP. Of note, ESO inhibited the progression into S and G2/M phase in a time-dependent manner, while ADM and DDP inhibited DNA synthesis by causing S-phase arrest in AGS cells. Omeprazole was reported to dose-dependently inhibit the growth of Barrett's esophagus and induce cell cycle arrest in G0/G1 phase (22). Pantoprazole treatment caused cell cycle arrest in G0/G1 phase to induce apoptosis in glioma cells (24). The different of structures of PPIs, cell lines and experimental conditions cannot be ruled out. After treatment with ESO, ADM and DDP, cells were distinctly accumulated in the S-phase. This phenomenon may be associated with the fact that PPIs reverse the pH gradient and assist the chemotherapeutic drugs to enter the cells, thus affecting the cell cycle (9,18). The present results suggested a role of PPIs in promoting apoptosis of GC cells, suggesting

further exploration of the anti-tumor mechanisms of ESO in preclinical studies.

Accumulating evidence indicated that dysregulation of lncRNAs, circRNAs, miRNAs and mRNAs contributes to the development and progression of GC (17,25). Based on lncRNA microarray, it was detected that the top 10 lncRNAs, circRNAs and mRNAs were mostly concentrated on chr10 and chr19. Cytochrome P450 family 1 subfamily A member 1 (CYP1A1), which is closely associated with the metabolism of PPIs (26), was upregulated 5-fold. At present, multiple chemotherapeutic drugs require metabolic activation by CYP1A1 to exert their cytostatic action (27). As a classic target gene of the Aryl hydrocarbon receptor pathway, upregulated CYP1A1 may mediate the growth and apoptosis in GC (28). It was hypothesized that CYP1A1 may be an important target of PPIs in GC to have antitumor effects. Among the genes detected on chr10, the downregulation of aldo-keto reductase family 1 member C1 significantly reversed oxaliplatin resistance in GC and ATP binding cassette subfamily C member 2-24C>T polymorphism was associated with the response to platinum/5-fluorouracil-based neoadjuvant chemotherapy in advanced GC (29,30). Furthermore, the present results revealed that deleted in malignant brain tumors 1 (DMBT1) was upregulated after ESO treatment. Paresi *et al* (31) revealed a potential link between benzimidazole compounds (the same effects as those of PPIs) and DMBT1 for *H. pylori* eradication and mucosal protection. Whether DMBT1 is a direct target of PPIs and has a specific regulatory mechanism remains to be further confirmed. Wang *et al* (32) suggested that chromosomal instability was associated with the aggressiveness of peritoneal metastasis in GC, such as chr19 gain. Therefore, it was speculated that chr10 and chr19 may be closely linked to the chemotherapy response and aggressiveness in GC, respectively. Thus, studies should further explore the associated genes on these chromosomes to identify relevant targets for the treatment of GC.

Apoptotic signaling pathway and DNA replication were pivotal terms accumulated by the up- and downregulated lncRNAs, respectively. In the category CC, altered lncRNAs were enriched in cytosol, extracellular exosome and nucleosome. KEGG pathway analysis indicated that EGFR tyrosine kinase inhibitor resistance and microRNAs in cancer were enriched by the upregulated lncRNAs. Cell cycle and DNA replication were significant among the downregulated lncRNAs, which were both enriched in the lncRNA/circRNA-miRNA-mRNA ceRNA networks. Exosomes are small vesicles containing multiple miRNAs and proteins. High doses of PPIs were observed to suppress the malignant features of GC via inhibiting the release of exosomes (23). Exosomes and miRNAs may be promising for the detection and acquisition of ideal biomarkers, and may provide a basis for novel therapeutic strategies in GC. In addition, it was inferred that ESO mainly suppressed GC progression by disrupting DNA synthesis and cell cycle progression, and promoting the apoptotic signaling pathway.

In terms of the classical tumor signaling pathways reported, such as the EGFR tyrosine kinase inhibitor resistance pathway and the FOXO signaling pathway, it was indicated that EGFR, FOXO3 and SOS1 were all upregulated after treatment with ESO. Of note, both FOXO3 and EGFR were targets of ENST00000613376, and lnc-endogenous retrovirus FRD 1-1:1(ERVFRD-1-1:1) was able to regulate FOXO3 and SOS1 simultaneously. FOXO3 overexpression and acidic stress have important roles in inducing apoptosis and autophagy in AGS cells via the PI3K/AKT signaling pathway (33). Knockdown of EGFR-antisense 1 inhibited cell proliferation by suppressing the EGFR-dependent PI3K/AKT pathway in GC (34). However, panaxydol exposure activated EGFR in MCF-7 cells, which triggered endoplasmic reticulum stress and induced cell apoptosis (35). As a regulator downstream of EGFR, FOXO3 was phosphorylated and degraded in colon cancer following EGFR activation (36). The SOS family mediates multiple signaling cascade connections. Growth factor receptor-bound protein 2 (GRB2) knockdown led to decreased phosphorylation of EGFR, and phosphorylated EGFR and the GRB2/SOS1 complex mediated resistance to osimertinib in acquired afatinib-resistant non-small cell lung cancer with sustained KRAS activation (37). Whether the upregulation of EGFR is related to the upregulation of SOS1 remains elusive. In addition, whether there is an antitumor effect by targeting ENST00000613376 or lnc-ERVFRD-1-1:1 to activate the EGFR/FOXO3/SOS1 signaling pathway remains to be explored.

The p53 pathway is associated with proliferation, apoptosis and cell cycle changes in cancer cells, which are regulated by multiple genes (38,39). Platinum drug resistance remains is an intractable challenge in anticancer treatment. Cell cycle arrest was indicated to be predominantly mediated by transcriptionally increased expression of growth arrest and DNA-damage-inducible 45 α (GADD45A) and CDKN1A, and by decreased SKP2 levels (40). MAPK1/3, BIRC5 and SKP2 have important roles in the apoptosis of osteosarcoma cells (40). It was proven that downregulation of BIRC5 (41), CCNB1 (38) and G2 and S phase-expressed-1 (GTSE-1) (42) has key roles in tumor inhibition. PMAIP1 belongs to the pro-apoptotic BH3-only family. It was reported that upregulated PMAIP1 has a crucial role in inducing apoptosis in bladder cancer (43). These results were consistent with those of the present study.

By integrating the lncRNA/circRNA-miRNA-mRNA co-expression networks, the complex ceRNA networks were constructed. In addition, there were two signaling pathways: NR_033268, ENST00000261530, ENST00000281092/hsa_circ_0076332, hsa_circ_0059713-hsa-miR-372-5p-MAP2, HIPK2 and ANK2. MAP2 is a novel prognostic marker in gemcitabine-resistant pancreatic cancer (44). HIPK family members are potent oncogenes and drive epithelial-to-mesenchymal transition. Overexpression of HIPK promoted excessive cell proliferation and invasion (45). Silencing of ANK2 restrained the migration and invasive potential of pancreatic carcinoma (46). Furthermore, miR-647 inhibited proliferation and metastasis in GC by downregulating ANK2 (47). Consequently, MAP2, HIPK2 and ANK2 may be important targets of ESO, exerting an anti-tumor effect in AGS cells. It was hypothesized that lncRNAs and circRNAs regulate mRNA expression and degradation through co-competition of miRNAs, and further affect the occurrence and development of tumors.

However, certain limitations of the present study should be considered. First, as activated prodrugs in an acidic

environment, PPIs inhibit the activity of H^+ and K^+-ATPase and induce cancer cell death by affecting pH homeostasis (48). However, various anti-cancer targets and mechanisms of PPIs also have been realized under neutral pH conditions (11,19-24). The objective of the present study was to explore the anti-GC effect of ESO repurposed as a chemical anti-cancer agent under normal culture conditions and to explore the underlying mechanisms. Whether PPIs have a similar impact on GC and associated mechanisms in a low-pH environment remains to be determined. The present data may provide a basis for additional experiments under different pH conditions. Furthermore, while the powerful anticancer effects of ESO have been demonstrated in mouse models of melanoma, the potency of ESO requires to be confirmed in GC in *in vivo* experiments (49). Finally, the potential therapeutic targets and signaling pathways determined in the present study require further verification. Therefore, validation experiments will be performed in the future in order to strengthen the support for the application of ESO as a clinical treatment.

In conclusion, the present results confirmed that ESO inhibits the proliferation, migration and invasion of AGS cells, while strongly enhancing the cells' chemosensitivity and inducing apoptosis by causing cell cycle arrest at the S and G2/M phases. Furthermore, the profiles of RNAs regulated by ESO, including lncRNAs, circRNAs, miRNAs and mRNAs, were determined for the first time, to the best of our knowledge. HIPK2, MAP2 and ANK2 may be valuable targets for diagnosis and treatment of GC. Furthermore, the EGFR tyrosine kinase inhibitor resistance pathway, FOXO signaling pathway, p53 signaling pathway and platinum drug resistance pathway may be closely associated with the antitumor effect of ESO in AGS cells, although its specific mechanism requires to be further verified in detail. These novel results enhance the current understanding of the complex molecular mechanisms of the effect of ESO on GC cell growth and provide prospective targets for gene therapy.

Acknowledgements

Not applicable.

Availability of data and materials

The datasets used and/or analyzed during the current study are available from the corresponding author on reasonable request.

Authors' contributions

ZZ and NB conceived and designed the study. QX and XJ wrote the manuscript and were responsible for cytological data analysis. QW performed the cytological experiments. QX, LS and XX were responsible for data analysis and interpretation of chip detection and RNA-sequencing data. LS and XX revised the initial manuscript critically for important intellectual content. ZM and HZ performed the acquisition and collation of data, contributed to the statistical analysis and plotted all statistical graphs and tables. ZZ, NB, LS and XX revised the manuscript and approved the final version of the manuscript submitted for publication. All authors read and approved the manuscript and agreed to be accountable for all aspects of the research in ensuring that the accuracy or integrity of any part of the work were appropriately investigated and resolved.

Ethics approval and consent to participate

Not applicable.

Patient consent for publication

Not applicable.

Competing interests

The authors declare that they have no competing interests.

References

1. Bray F, Ferlay J, Soerjomataram I, Siegel RL, Torre LA and Jemal A: Global cancer statistics 2018: GLOBOCAN estimates of incidence and mortality worldwide for 36 cancers in 185 countries. CA Cancer J Clin 68: 394-424, 2018.
2. Ilson DH: Advances in the treatment of gastric cancer. Curr Opin Gastroenterol 33: 473-476, 2017.
3. Giustini NP, Jeong AR, Buturla J and Bazhenova L: Advances in treatment of locally advanced or metastatic Non-Small cell lung cancer: Targeted Therapy. Clin Chest Med 41: 223-235, 2020.
4. Song YH, He L, Wang YL, Wu Q and Huang WZ: Molecularly targeted therapy and immunotherapy for hormone Receptor-positive/human epidermal growth factor receptor 2-negative advanced breast cancer (Review). Oncol Rep 44: 3-13, 2020.
5. Kinoshita Y, Ishimura N and Ishihara S: Advantages and disadvantages of Long-term proton pump inhibitor use. J Neurogastroenterol Motil 24: 182-196, 2018.
6. Ikemura K, Hiramatsu S and Okuda M: Drug repositioning of proton pump inhibitors for enhanced efficacy and safety of cancer chemotherapy. Front Pharmacol 8: 911, 2017.
7. Watanabe SM, Ehrlich LS, Strickland M, Li X, Soloveva V, Goff AJ, Stauft CB, Bhaduri-McIntosh S, Tjandra N and Carter C: Selective targeting of virus replication by proton pump inhibitors. Sci Rep 10: 4003, 2020.
8. Fako VE, Wu X, Pflug B, Liu JY and Zhang JT: Repositioning proton pump inhibitors as anticancer drugs by targeting the thioesterase domain of human fatty acid synthase. J Med Chem 58: 778-784, 2015.
9. Lu ZN, Tian B and Guo XL: Repositioning of proton pump inhibitors in cancer therapy. Cancer Chemother Pharmacol 80: 925-937, 2017.
10. Lindner K, Borchardt C, Schöpp M, Bürgers A, Stock C, Hussey DJ, Haier J and Hummel R: Proton pump inhibitors (PPIs) impact on tumour cell survival, metastatic potential and chemotherapy resistance, and affect expression of resistance-relevant miRNAs in esophageal cancer. J Exp Clin Cancer Res 33: 73, 2014.
11. He J, Shi XY, Li ZM, Pan XH, Li ZL, Chen Y, Yan SJ and Xiao L: Proton pump inhibitors can reverse the YAP mediated paclitaxel resistance in epithelial ovarian cancer. BMC Mol Cell Biol 20: 49, 2019.
12. Ransohoff JD, Wei Y and Khavari PA: The functions and unique features of long intergenic Non-coding RNA. Nat Rev Mol Cell Biol 19: 143-157, 2018.
13. Li Y, Ge YZ, Xu L and Jia R: Circular RNA ITCH: A novel tumor suppressor in multiple cancers. Life Sci 254: 117176, 2020.
14. Hausser J and Zavolan M: Identification and consequences of miRNA-target Interactions-beyond repression of gene expression. Nat Rev Genet 15: 599-612, 2014.

15. Huang M, Zhong Z, Lv M, Shu J, Tian Q and Chen J: Comprehensive analysis of differentially expressed profiles of lncRNAs and circRNAs with associated co-expression and ceRNA networks in bladder carcinoma. Oncotarget 7: 47186-47200, 2016.
16. Zhu J, Zhang X, Gao W, Hu H, Wang X and Hao D: lncRNA/circRNA-miRNA-mRNA ceRNA network in lumbar intervertebral disc degeneration. Mol Med Report 20: 3160-3174, 2019.
17. Li J, Wang X, Lu W, Xiao Y, Yu Y, Wang X, Xu C and Shen B: Comprehensive analysis of differentially expressed Non-coding RNAs and mRNAs in gastric cancer cells under hypoxic conditions. Am J Transl Res 10: 1022-1035, 2018.
18. Iessi E, Logozzi M, Mizzoni D, Di Raimo R, Supuran CT and Fais S: Rethinking the combination of proton exchanger inhibitors in cancer therapy. Metabolites 8: 2, 2018.
19. Zhang B, Ling T, Zhaxi P, Cao Y, Qian L, Zhao D, Kang W, Zhang W, Wang L, Xu G and Zou X: Proton pump inhibitor pantoprazole inhibits gastric cancer metastasis via suppression of telomerase reverse transcriptase gene expression. Cancer Lett 452: 23-30, 2019.
20. Marino ML, Fais S, Djavaheri-Mergny M, Villa A, Meschini S, Lozupone F, Venturi G, Della Mina P, Pattingre S, Rivoltini L, et al: Proton pump inhibition induces autophagy as a survival mechanism following oxidative stress in human melanoma cells. Cell Death Dis 1: e87, 2010.
21. Cao Y, Chen M, Tang D, Yan H, Ding X, Zhou F, Zhang M, Xu GF, Zhang W, Zhang S, et al: The proton pump inhibitor pantoprazole disrupts protein degradation systems and sensitizes cancer cells to death under various stresses. Cell Death Dis 9: 604, 2018.
22. Hou Y, Hu Q, Huang J and Xiong H: Omeprazole inhibits cell proliferation and induces G0/G1 cell cycle arrest through Up-regulating miR-203a-3p expression in barrett's esophagus cells. Front Pharmacol 8: 968, 2017.
23. Guan XW, Zhao F, Wang JY, Wang HY, Ge SH, Wang X, Zhang L, Liu R, Ba Y, Li HL, et al: Tumor microenvironment interruption: A novel Anti-cancer mechanism of Proton-pump inhibitor in gastric cancer by suppressing the release of microRNA-carrying exosomes. Am J Cancer Res 7: 1913-1925, 2017.
24. Geeviman K, Babu D and Prakash Babu P: Pantoprazole induces mitochondrial apoptosis and attenuates NF-κB signaling in glioma cells. Cell Mol Neurobiol 38: 1491-1504, 2018.
25. Zhang Y, Han T, Li J, Cai H, Xu J, Chen L and Zhan X: Comprehensive analysis of the regulatory network of differentially expressed mRNAs, lncRNAs and circRNAs in gastric cancer. Biomed Pharmacother 122: 109686, 2020.
26. Wu D, Qiu T, Zhang Q, Kang H, Yuan S, Zhu L and Zhu R: Systematic toxicity mechanism analysis of proton pump inhibitors: An in silico study. Chem Res Toxicol 28: 419-430, 2015.
27. Mescher M and Haarmann-Stemmann T: Modulation of CYP1A1 metabolism: From adverse health effects to chemoprevention and therapeutic options. Pharmacol Ther 187: 71-87, 2018.
28. Yin XF, Chen J, Mao W, Wang YH and Chen MH: A selective aryl hydrocarbon receptor modulator 3,3'-Diindolylmethane inhibits gastric cancer cell growth. J Exp Clin Cancer Res 31: 46, 2012.
29. Chen CC, Chu CB, Liu KJ, Huang CY, Chang JY, Pan WY, Chen HH, Cheng YH, Lee KD, Chen MF, et al: Gene expression profiling for analysis acquired oxaliplatin resistant factors in human gastric carcinoma TSGH-S3 cells: The role of IL-6 signaling and Nrf2/AKR1C axis identification. Biochem Pharmacol 86: 872-887, 2013.
30. Li Z, Xing X, Shan F, Li S, Li Z, Xiao A, Xing Z, Xue K, Li Z, Hu Y, et al: ABCC2-24C>T polymorphism is associated with the response to platinum/5-Fu-based neoadjuvant chemotherapy and better clinical outcomes in advanced gastric cancer patients. Oncotarget 7: 55449-55457, 2016.
31. Paresi CJ, Liu Q and Li YM: Benzimidazole covalent probes and the gastric H(+)/K(+)-ATPase as a model system for protein labeling in a Copper-free setting. Mol Biosyst 12: 1772-1780, 2016.
32. Wang R, Song S, Harada K, Ghazanfari Amlashi F, Badgwell B, Pizzi MP, Xu Y, Zhao W, Dong X, Jin J, et al: Multiplex profiling of peritoneal metastases from gastric adenocarcinoma identified novel targets and molecular subtypes that predict treatment response. Gut 69: 18-31, 2020.
33. Gao Y, Qi W, Sun L, Lv J, Qiu W and Liu S: FOXO3 Inhibits human gastric adenocarcinoma (AGS) cell growth by promoting autophagy in an acidic microenvironment. Cell Physiol Biochem 49: 335-348, 2018.
34. Hu J, Qian Y, Peng L, Ma L, Qiu T, Liu Y, Li X and Chen X: Long noncoding RNA EGFR-AS1 promotes cell proliferation by increasing EGFR mRNA stability in gastric cancer. Cell Physiol Biochem 49: 322-334, 2018.
35. Kim HS, Lim JM, Kim JY, Kim Y, Park S and Sohn J: Panaxydol, a component of Panax ginseng, induces apoptosis in cancer cells through EGFR activation and ER stress and inhibits tumor growth in mouse models. Int J Cancer 138: 1432-1441, 2016.
36. Qi W, Weber CR, Wasland K, Roy H, Wali R, Joshi S and Savkovic SD: Tumor suppressor FOXO3 mediates signals from the EGF receptor to regulate proliferation of colonic cells. Am J Physiol Gastrointest Liver Physiol 300: G264-G272, 2011.
37. Nakatani K, Yamaoka T, Ohba M, Fujita KI, Arata S, Kusumoto S, Taki-Takemoto I, Kamei D, Iwai S, Tsurutani J and Ohmori T: KRAS and amplifications mediate resistance to rociletinib and osimertinib in acquired afatinib-resistant NSCLC harboring exon 19 deletion/T790M in EGFR. Mol Cancer Ther 18: 112-126, 2019.
38. Zhang H, Zhang X, Li X, Meng WB, Bai ZT, Rui SZ, Wang ZF, Zhou WC and Jin XD: Effect of CCNB1 silencing on cell cycle, senescence, and apoptosis through the p53 signaling pathway in pancreatic cancer. J Cell Physiol 234: 619-631, 2018.
39. Wei GH and Wang X: lncRNA MEG3 inhibit proliferation and metastasis of gastric cancer via p53 signaling pathway. Eur Rev Med Pharmacol Sci 21: 3850-3856, 2017.
40. Kleinsimon S, Longmuss E, Rolff J, Jäger S, Eggert A, Delebinski C and Seifert G: GADD45A and CDKN1A are involved in apoptosis and cell cycle modulatory effects of viscumTT with further inactivation of the STAT3 pathway. Sci Rep 8: 5750, 2018.
41. Shang X, Liu G, Zhang Y, Tang P, Zhang H, Jiang H and Yu Z: Downregulation of BIRC5 inhibits the migration and invasion of esophageal cancer cells by interacting with the PI3K/Akt signaling pathway. Oncol Lett 16: 3373-3379, 2018.
42. Guo L, Zhang S, Zhang B, Chen W, Li X, Zhang W, Zhou C, Zhang J, Ren N and Ye Q: Silencing GTSE-1 expression inhibits proliferation and invasion of hepatocellular carcinoma cells. Cell Biol Toxicol 32: 263-274, 2016.
43. Cui J, Sun W, Hao X, Wei M, Su X, Zhang Y, Su L and Liu X: EHMT2 inhibitor BIX-01294 induces apoptosis through PMAIP1-USP9X-MCL1 axis in human bladder cancer cells. Cancer Cell Int 15: 4, 2015.
44. Le Large TYS, El Hassouni B, Funel N, Kok B, Piersma SR, Pham TV, Olive KP, Kazemier G, van Laarhoven HWM, Jimenez CR, et al: Proteomic analysis of gemcitabine-resistant pancreatic cancer cells reveals that microtubule-associated protein 2 upregulation associates with taxane treatment. Ther Adv Med Oncol 11: 1758835919841233, 2019.
45. Blaquiere JA, Wong KKL, Kinsey SD, Wu J and Verheyen EM: Homeodomain-interacting protein kinase promotes tumorigenesis and metastatic cell behavior. Dis Model Mech 11: dmm031146, 2018.
46. Chen Y, Löhr M and Jesnowski R: Inhibition of ankyrin-B expression reduces growth and invasion of human pancreatic ductal adenocarcinoma. Pancreatology 10: 586-596, 2010.
47. Cao W, Wei W, Zhan Z, Xie D, Xie Y and Xiao Q: Role of miR-647 in human gastric cancer suppression. Oncol Rep 37: 1401-1411, 2017.
48. Mullin JM, Gabello M, Murray LJ, Farrell CP, Bellows J, Wolov KR, Kearney KR, Rudolph D and Thornton JJ: Proton pump inhibitors: Actions and reactions. Drug Discov Today 14: 647-660, 2009.
49. De Milito A, Canese R, Marino ML, Fais S, Venturi G, Rodolfo M, Borghi M, Villa A, Della Mina P, Lozupone F, et al: pH-dependent antitumor activity of proton pump inhibitors against human melanoma is mediated by inhibition of tumor acidity. Int J Cancer 127: 207-219, 2010.